Control of Axial Ligand Substitution in *trans*-Bis(2,2′-bipyridine)ruthenium(II) Complexes. Crystal and Molecular Structure of *trans*-(4-Ethylpyridine)(dimethyl sulfoxide)-bis(2,2′-bipyridine)ruthenium(II) Hexafluorophosphate, *trans*-$[Ru(bpy)_2(4\text{-}Etpy)(DMSO)](PF_6)_2$

Benjamin J. Coe,* Thomas J. Meyer, and Peter S. White

Department of Chemistry, The University of North Carolina, Chapel Hill, North Carolina 27599-3290

*Received April 1, 1993**

The ruthenium(II) complex in the salt *trans*-$[Ru(bpy)_2(H_2O)_2](CF_3SO_3)_2$ (bpy = 2,2′-bipyridine) is converted quantitatively into the corresponding bis-DMSO complex by reaction at ambient temperature in DMSO and is isolated as the salt *trans*-$[Ru(bpy)_2(DMSO)_2](CF_3SO_3)_2 \cdot 0.5H_2O$ (**1**). **1** reacts with a pyridyl ligand in DMSO at ambient temperature to give *trans*-$[Ru(bpy)_2(py)(DMSO)](PF_6)_2 \cdot nH_2O$ (py = 4-ethylpyridine (4-Etpy), $n = 0$ (**2**); py = 4-(dimethylamino)pyridine (DMAP), $n = 1.5$ (**3**); py = ethyl isonicotinate (ISNE), $n = 1$ (**4**)). The single-crystal X-ray structure of *trans*-$[Ru(bpy)_2(4\text{-}Etpy)(DMSO)](PF_6)_2 \cdot 0.5DMF$ (**2**·0.5DMF) has been determined. This salt crystallizes in the monoclinic system, space group $P2_1/c$ with $a = 15.0301(9)$ Å, $b = 18.1948(12)$ Å, $c = 14.6323(7)$ Å, $\beta = 97.769(5)°$, and $Z = 4$. The DMSO molecule is S-bound. **2** is converted into *trans*-$[Ru(bpy)_2(4\text{-}Etpy)Cl]PF_6 \cdot H_2O$ (**5**) by reaction with LiCl in DMF/water at elevated temperature. Removal of the chloride ligand in **5** by $AgCF_3CO_2$ in acetone/water at room temperature in the presence of a second pyridyl ligand (ISNE) affords a mixed-pyridine complex which is isolated in nearly quantitative yield as the salt *trans*-$[Ru(bpy)_2(4\text{-}Etpy)(ISNE)](PF_6)_2$ (**6**).

Introduction

Ruthenium and osmium polypyridyl complexes have well-established redox and photophysical properties[1] and are currently receiving considerable attention as candidates for incorporation into photochemical molecular devices.[2] The vast majority of work to date in this area has involved tris(2,2′-bipyridyl) or bis(2,2′-bipyridyl) complexes having the cis geometry. These complexes show high stability and are synthetically readily accessible.[3] Recent noteworthy reports have detailed the preparation and photophysical properties of high-nuclearity supramolecular *cis*-$Ru(bpy)_2^{2+}$-based structures by using 2,3-bis(2-pyridyl)pyrazine as a bridging ligand in a stepwise synthetic strategy.[4]

An important aspect of the coordination chemistry of the tris-(2,2′-bipyridyl) and *cis*-bis(2,2′-bipyridyl) complexes is the low degree of stereochemical control inherent in their preparation. Both optical isomerism and, with asymmetrically substituted bpy ligands, structural isomerism can occur. Little or no synthetic control over isomer formation is available, and separation techniques are not yet at the stage where the various isomers can be resolved. The existence of unresolved isomers sets significant limitations upon the level of understanding available in the interpretation of photophysical and related properties.

One approach to the construction of ruthenium bpy complex arrays in which charge- and energy-transfer processes could be exploited to their greatest effect is to synthesize species bearing trans substituents. This might be realized by the manipulation of the axial ligands in complexes containing the *trans*-$[Ru(bpy)_2]^{2+}$ core. A system which represents a likely candidate for the synthesis of functionalized ruthenium(II) trans complexes is *trans*-$[Ru(bpy)_2(X)(Y)]^{n+}$ (X, Y = pyridine, acetonitrile, *etc.*; $n = 1, 2$).[5] Previous work with such complexes has involved only the preparation of symmetrical (X = Y) or randomly produced asymmetrical derivatives, and in order to proceed, it is necessary to develop a rational strategy for the stepwise attachment of selected trans ligands. Two precursors which are attractive at first glance are *trans*-$[Ru(bpy)_2(H_2O)_2](CF_3SO_3)_2$[6] and *trans*-$Ru(bpy)_2Cl_2$.[5] However, the latter complex is insoluble in all common solvents, which effectively precludes its use as a synthetic precursor. Hence the diaquo complex has been chosen as the most promising starting material for this study.

Previous reports have demonstrated controlled asymmetrical trans substitution with pyridyl ligands in complexes of the form *trans*-$[Ru(NH_3)_4(L)(L')]^{n+}$ (for example: L = pyridine, L′ = pyrazine, $n = 2$;[7] L = imidazole, L′ = isonicotinamide, $n = 3$[8]). However, the precursor for these syntheses, *trans*-$[Ru(NH_3)_4(SO_2)Cl]^+$,[9] has no known analogue in *trans*-$[Ru(bpy)_2(X)(Y)]^{n+}$ chemistry. In the field of macrocyclic chemistry, the fixed trans geometry in octahedral complexes of unsaturated N_4 macrocycles was recently exploited to prepare complexes of the form $[Ru(TZ)(X)(Y)]^{2+}$ (TZ = 2,7,12,17-tetramethyl-1,6,11,16-tetraazaporphyrinogen; X = DMSO, Y = DMSO or pyridine; X = CH_3CN, Y = CH_3CN or pyridine; X = Y = pyridine or 4,4′-

* Abstract published in *Advance ACS Abstracts,* August 15, 1993.

(1) (a) Sutin, N.; Creutz, C. *Pure Appl. Chem.* **1980**, *52*, 2717. (b) Durham, B.; Caspar, J. V.; Nagle, J. K.; Meyer, T. J. *J. Am. Chem. Soc.* **1982**, *104*, 4803. (c) Krause, R. A. *Struct. Bonding (Berlin)* **1987**, *67*, 1. (d) Juris, A.; Balzani, V.; Barigelletti, F.; Campagna, S.; Belser, P.; von Zelewsky, A. *Coord. Chem. Rev.* **1988**, *84*, 85. (e) Kober, E. M.; Caspar, J. V.; Sullivan, B. P.; Meyer, T. J. *Inorg. Chem.* **1988**, *27*, 4587. (f) Meyer, T. J. *Acc. Chem. Res.* **1989**, *22*, 163. (g) Meyer, T. J. *Pure Appl. Chem.* **1990**, *62*, 1003. (h) Nagle, J. K.; Roundhill, D. M. *Chemtracts: Inorg. Chem.* **1992**, *4*, 141.

(2) Balzani, V.; Scandola, F. *Supramolecular Photochemistry*; Ellis Horwood: Chichester, U.K., 1991.

(3) See for example: (a) Godwin, J. B.; Meyer, T. J. *Inorg. Chem.* **1971**, *10*, 471. (b) Adeyemi, S. A.; Miller, F. J.; Meyer, T. J. *Inorg. Chem.* **1972**, *11*, 994. (c) Callahan, R. W.; Meyer, T. J. *Inorg. Chem.* **1977**, *16*, 574. (d) Pinnick, D. V.; Durham, B. *Inorg. Chem.* **1984**, *23*, 1440. (e) Danielson, E.; Elliott, C. M.; Merkert, J. W.; Meyer, T. J. *J. Am. Chem. Soc.* **1987**, *109*, 2519. (f) Rillema, D. P.; Blanton, C. B.; Shaver, R. J.; Jackman, D. C.; Boldaji, M.; Bundy, S.; Worl, L. A.; Meyer, T. J. *Inorg. Chem.* **1992**, *31*, 1600.

(4) (a) Campagna, S.; Denti, G.; Serroni, S.; Ciano, M.; Balzani, V. *J. Am. Chem. Soc.* **1992**, *114*, 2944. (b) Campagna, S.; Denti, G.; Serroni, S.; Ciano, M.; Juris, A.; Balzani, V. *Inorg. Chem.* **1992**, *31*, 2982.

(5) Walsh, J. L.; Durham, B. *Inorg. Chem.* **1982**, *21*, 329.

(6) (a) Dobson, J. C.; Meyer, T. J. *Inorg. Chem.* **1988**, *27*, 3283. (b) Coe, B. J.; Thompson, D. W. Unpublished results.

(7) Tfouni, E.; Ford, P. C. *Inorg. Chem.* **1980**, *19*, 72.

(8) Wishart, J. F.; Zhang, X.; Isied, S. S.; Potenza, J. A.; Schugar, H. J. *Inorg. Chem.* **1992**, *31*, 3179.

(9) Isied, S. S.; Taube, H. *Inorg. Chem.* **1974**, *13*, 1545.

0020-1669/93/1332-4012$04.00/0

bipyridine).[10] The achievement of asymmetrical substitution by using $[Ru(TZ)(DMSO)_2](PF_6)_2$ as a precursor demonstrates a strategy which may have potential application to *trans*-$[Ru(bpy)_2(X)(Y)]^{n+}$ complexes. The most significant limiting factor in this approach is likely to be the strong tendency for isomerization to the more stable cis form, which cannot occur in complexes of a sufficiently unsaturated macrocycle such as TZ. Furthermore, trans effects will be of crucial importance in influencing substitution chemistry.

Experimental Section

Materials and Procedures. The salt *trans*-$[Ru(bpy)_2(H_2O)_2](CF_3SO_3)_2$ was prepared by using a modification of a previously published procedure.[6] All other reagents were obtained commercially and used as supplied. All reactions were carried out in the dark under an atmosphere of argon. Products were dried at room temperature in a vacuum desiccator for periods of *ca.* 15 h prior to characterization. A common tendency to retain water in the solid state has previously been documented for *cis*-$Ru(bpy)_2^{2+}$ complexes.[3a]

Physical Measurements. ^1H NMR spectra were recorded on a Bruker AC200 spectrometer, and all shifts are referenced to TMS. IR spectra were obtained as KBr disks with a Mattson Galaxy Series FTIR 5000 instrument. UV–visible spectra were recorded by using a Hewlett Packard 8451A diode array spectrophotometer. Elemental analyses were performed by ORS, Whitesboro, NY. Electrochemical measurements were made with a PAR Model 173 potentiostat with a PAR Model 175 universal programmer. Owing to the light-sensitive nature of the complexes, all solution measurements were carried out in the dark.

Synthesis of *trans*-$[Ru(bpy)_2(DMSO)_2](CF_3SO_3)_2\cdot 0.5H_2O$ (1). A solution of *trans*-$[Ru(bpy)_2(H_2O)_2](CF_3SO_3)_2$ (1.00 g, 1.34 mmol) in DMSO (7 mL) was stirred at room temperature for 48 h. Methanol (10 mL) was added, and the resulting yellow solution was poured into diethyl ether (500 mL). The mixture was cooled in a refrigerator for 2 h to ensure complete precipitation, and the product was collected by filtration. The bright yellow powder was washed several times with diethyl ether and dried: yield 1.16 g, 99%; δ_H (CD_3OD) 9.49 (4 H, dd, J = 5.1, 0.6 Hz, *bpy* × 2), 8.75 (4 H, dd, J = 8.2, 1.0 Hz, *bpy* × 2), 8.39 (4 H, td, J = 7.9, 1.4 Hz, *bpy* × 2), 7.93 (4 H, td, J = 6.7, 1.4 Hz, *bpy* × 2), 2.62 (6 H, *s*, Me_2SO). Anal. Calcd for $C_{26}H_{28}F_6N_4O_8RuS_4\cdot 0.5H_2O$: C, 35.61; H, 3.33; N, 6.39. Found: C, 35.52; H, 3.15; N, 6.33.

Synthesis of *trans*-$[Ru(bpy)_2(4\text{-}Etpy)(DMSO)](PF_6)_2$ (2). A solution of **1** (500 mg, 0.570 mmol) and 4-ethylpyridine (4-Etpy) (0.5 mL) in DMSO (4 mL) was stirred at room temperature for 15 h. The addition of aqueous NH_4PF_6 afforded a yellow precipitate, which was collected by filtration, washed with water followed by diethyl ether, and then dried: yield 501 mg, 99%; δ_H (CD_3SOCD_3) 9.65 (4 H, d, J = 5.5 Hz, *bpy* × 2), 8.61 (4 H, d, J = 8.0 Hz, *bpy* × 2), 8.32 (4 H, t, J = 7.7 Hz, *bpy* × 2), 7.95 (4 H, t, J = 6.4 Hz, *bpy* × 2), 7.60 (2 H, d, J = 6.0 Hz, *py*-Et), 6.96 (2 H, d, J = 5.9 Hz, *py*-Et), 2.57 (6 H, s, Me_2SO), 2.42 (2 H, q, J = 7.6 Hz, py–CH_2–Me), 0.92 (3 H, t, J = 7.5 Hz, $pyCH_2$–Me). Anal. Calcd for $C_{29}H_{31}F_{12}N_5OP_2RuS$: C, 39.20; H, 3.52; N, 7.88. Found: C, 38.94; H, 3.44; N, 7.80.

Synthesis of *trans*-$[Ru(bpy)_2(DMAP)(DMSO)](PF_6)_2\cdot 1.5H_2O$ (3). This complex was prepared identically to **2** by using **1** (50 mg, 0.057 mmol), 4-(dimethylamino)pyridine (DMAP) (80 mg, 0.655 mmol) in place of 4-ethylpyridine, and DMSO (3 mL). This afforded the product as a golden powder: yield 52 mg, 98%; δ_H (CD_3SOCD_3) 9.62 (4 H, d, J = 5.5 Hz, *bpy* × 2), 8.62 (4 H, d, J = 7.9 Hz, *bpy* × 2), 8.31 (4 H, t, J = 7.7 Hz, *bpy* × 2), 7.92 (4 H, t, J = 6.3 Hz, *bpy* × 2), 6.92 (2 H, d, J = 7.0 Hz, *py*–NMe_2), 6.14 (2 H, d, J = 7.1 Hz, *py*–NMe_2), 2.73 (6 H, s, py–NMe_2), 2.59 (6 H, s, Me_2SO). Anal. Calcd for $C_{29}H_{32}F_{12}N_6OP_2RuS\cdot 1.5H_2O$: C, 37.43; H, 3.79; N, 9.03. Found: C, 37.48; H, 3.45; N, 8.95.

Synthesis of *trans*-$[Ru(bpy)_2(ISNE)(DMSO)](PF_6)_2\cdot H_2O$ (4). This complex was prepared identically to **2** by using **1** (100 mg, 0.114 mmol), ethyl isonicotinate (ISNE) (0.5 mL) in place of 4-ethylpyridine, and DMSO (1.5 mL). This afforded the product as a yellow powder: yield 107 mg, 99%; δ_H (CD_3SOCD_3) 9.65 (4 H, d, J = 5.5 Hz, *bpy* × 2), 8.60 (4 H, d, J = 7.6 Hz, *bpy* × 2), 8.33 (4 H, t, J = 7.6 Hz, *bpy* × 2), 8.00–7.95 (6 H, m, *bpy* × 2, *py*–CO_2Et), 7.45 (2 H, d, J = 6.5 Hz, *py*–CO_2Et), 4.18 (2 H, q, J = 7.1 Hz, $pyCO_2$–CH_2–Me), 2.60 (6 H, s, Me_2SO), 1.16 (3 H, t, J = 7.1 Hz, $pyCO_2CH_2$–Me); ν(CO) 1725 (m), $\nu(PF_6)$ 860 (s) cm^{-1}. Anal. Calcd for $C_{30}H_{31}F_{12}N_5O_3P_2RuS\cdot H_2O$: C, 37.90; H, 3.50; N, 7.37. Found: C, 37.97; H, 3.37; N, 7.21.

Synthesis of *trans*-$[Ru(bpy)_2(4\text{-}Etpy)Cl]PF_6\cdot H_2O$ (5). **2** (294 mg, 0.331 mmol) was added to a saturated solution of LiCl in 1:1 (v/v) DMF/water (10 mL), and the mixture was heated at 105 °C for 2 h. The reaction mixture was cooled to room temperature, and water (40 mL) was added. The dark purple solid was collected by filtration, washed several times with water, and dried: yield 153 mg, 64%; δ_H (CD_3SOCD_3) 9.53 (4 H, d, J = 5.4 Hz, *bpy* × 2), 8.60 (4 H, d, J = 7.9 Hz, *bpy* × 2), 8.13 (4 H, t, J = 7.6 Hz, *bpy* × 2), 7.76 (4 H, t, J = 6.4 Hz, *bpy* × 2), 7.61 (2 H, d, J = 6.3 Hz, *py*–Et), 6.83 (2 H, d, J = 6.2 Hz, *py*–Et), 2.36 (2 H, q, J = 7.5 Hz, py–CH_2–Me), 0.91 (3 H, t, J = 7.5 Hz, $pyCH_2$–Me). Anal. Calcd for $C_{27}H_{25}ClF_6N_5PRu\cdot H_2O$: C, 45.10; H, 3.78; N, 9.74. Found: C, 45.42; H, 3.46; N, 9.56.

Synthesis of *trans*-$[Ru(bpy)_2(4\text{-}Etpy)(ISNE)](PF_6)_2$ (6). A solution of **5** (60 mg, 0.083 mmol), $AgCF_3CO_2$ (48 mg, 0.217 mmol), and ISNE (1 mL) in 40% aqueous acetone (15 mL) was stirred at room temperature for 72 h. The addition of aqueous NH_4PF_6 afforded an orange precipitate, which was collected by filtration (together with the AgCl) and washed several times with water. The product was redissolved through the frit in DMF (1.5 mL) and precipitated by the addiition of diethyl ether. The red-orange solid was collected by filtration, washed with diethyl ether, and then dried: yield 78 mg, 98%; δ_H (CD_3SOCD_3) 9.62 (4 H, d, J = 5.4 Hz, *bpy* × 2), 8.65 (4 H, d, J = 7.4 Hz, *bpy* × 2), 8.22 (4 H, t, J = 7.4 Hz, *bpy* × 2), 8.00 (2 H, dd, J = 5.5, 1.3 Hz, *py*–CO_2Et), 7.85 (4 H, t, J = 6.2 Hz, *bpy* × 2), 7.66 (2 H, d, J = 6.5 Hz, *py*–Et), 7.38 (2 H, dd, J = 5.4, 1.3 Hz, *py*–CO_2Et), 6.91 (2 H, d, J = 6.5 Hz, *py*–Et), 4.19 (2 H, q, J = 7.1 Hz, $pyCO_2$–CH_2–Me), 2.42 (2 H, q, J = 7.6 Hz, py–CH_2–Me), 1.17 (3 H, t, J = 7.1 Hz, $pyCO_2CH_2$–Me), 0.93 (3 H, t, J = 7.5 Hz, $pyCH_2$–Me); ν(CO) 1728 (m), $\nu(PF_6)$ 839 (s) cm^{-1}. Anal. Calcd for $C_{35}H_{34}F_{12}N_6O_2P_2Ru$: C, 43.71; H, 3.56; N, 8.74. Found: C, 43.48; H, 3.54; N, 8.60.

X-ray Structural Determination. Suitable crystals of **2** were grown by slow diffusion of diethyl ether vapor into a DMF solution at room temperature. A golden crystal of dimensions 0.25 × 0.25 × 0.15 mm was selected for diffraction study. Data were collected on a Rigaku AFC6/S diffractometer using the $\theta/2\theta$ scan mode with graphite-monochromated Mo Kα radiation (λ = 0.710 73 Å). Crystallographic data and refinement details are presented in Table II. A total of 84 high-angle reflections, $30.00 \le 2\theta \le 38.00°$, were used in a least-squares fit to obtain accurate cell constants. Of the 5152 unique reflections measured, 3461 reflections with $I > 2.5\sigma(I)$ were used in the structure solution and subsequent refinement. Final agreement indices of R = 6.5% and R_w = 8.4% resulted with hydrogen atoms placed in their calculated positions. Weights were estimated from counter statistics. In the case of the CH_3 groups, these were defined as rigid bodies and permitted to rotate at an intermediate point in the refinement to optimize their orientation.

Both PF_6 counterions are disordered and are modeled with 12 F positions each with occupancies adding up correctly. As a result, the F thermal parameters are probably meaningless. The crystal contains 0.5 molecules of DMF per asymmetric unit. No correction was made for absorption. ORTEP[11] diagrams showing two views of the cation are given in Figure 3. Selected bond distances are given in Table III, selected bond angles in Table IV, and final atomic fractional coordinates in Table V. Anisotropic thermal parameters, hydrogen atomic parameters, and all nonessential bond lengths and angles are provided as supplementary material. All computations were performed by using the NRCVAX[12] suite of programs. Atomic scattering factors were taken from a standard source[13] and corrected for anomalous dispersion.

Results and Discussion

Synthetic Studies. The reaction of *trans*-$[Ru(bpy)_2(H_2O)_2](CF_3SO_3)_2$ with DMSO proceeds relatively rapidly at room temperature to form quantitatively the corresponding *trans*-bis(dimethyl sulfoxide) complex, which is isolated as the salt *trans*-$[Ru(bpy)_2(DMSO)_2](CF_3SO_3)_2\cdot 0.5H_2O$ (**1**). No evidence for

(10) (a) Marzin, C.; Tarrago, G.; Gal, M.; Zidane, I.; Hours, T.; Lerner, D.; Andrieux, C.; Gampp, H.; Saveant, J. M. *Inorg. Chem.* **1986**, *25*, 1775. (b) Marzin, C.; Tarrago, G.; Zidane, I.; Bienvenue, E.; Seta, P.; Andrieux, C.; Gampp, H.; Saveant, J. M. *Inorg. Chem.* **1986**, *25*, 1778.

(11) Johnson, C. K. ORTEP: A Fortran thermal ellipsoid plot program; Technical Report ORNL-5138; Oak Ridge National Laboratory: Oak Ridge, TN, 1976.

(12) Gabe, E. J.; Le Page, Y.; Charland, J.-P.; Lee, F. L.; White, P. S. *J. Appl. Crystallogr.* **1989**, *22*, 384.

(13) *International Tables for X-ray Crystallography*; Kynoch Press: Birmingham, U.K., 1974; Vol. IV.

Table I. Spectral and Electrochemical Data for the Salts *trans*-$[Ru(bpy)_2(X)(Y)](Z)_n$

no.	X	Y	Z	*n*	λ_{max}, nm (ϵ, M^{-1} cm^{-1})[a]	$E_{1/2}$, V (ΔE_p, mV)[b] initial or $E_{p,a}$	after oxidation	after photolysis[e]
1	DMSO	DMSO	OTf	2	292 (31 900) 420 (6900)	1.62[c]	1.09 (110) 0.69 (100)	1.47 (115)
2	4-Etpy	DMSO	PF_6	2	290 (39 500) 416 (8700)	1.77[c]	1.33 (110) 0.99 (100)	1.36 (100)
3	DMAP	DMSO	PF_6	2	292 (60 400) 434 (8500)	1.47[c]	0.78 (100)	1.13 (100)
4	ISNE	DMSO	PF_6	2	288 (33 500) 410 (8200)	1.83[c]	1.41 (115) 1.07 (110)	1.44 (125)[d]
5	4-Etpy	Cl	PF_6	1	262 (14 800) 304 (37 800) 372 (11 200) 520 (10 900) 544 (10 300)	0.72 (100)		0.86 (105)
6	4-Etpy	ISNE	PF_6	2	262 (18 700) 298 (41 700) 383 (9900) 478 (13 700)	1.29 (105)		1.35 (130)[d]

[a] Spectra recorded at ambient temperature in DMSO solution at concentrations of *ca.* 10^{-5} M. [b] Recorded at ambient temperature in acetonitrile solution 0.1 M in $[N(C_4H_9\text{-}n)_4][PF_6]$ at a Pt disk working electrode (surface area 0.031 cm^2) with a scan rate of 200 mV s^{-1}. All potentails are vs SCE. Ferrocene internal reference $E_{1/2}$ = 0.41 V, ΔE_p = 100 mV. Solutions *ca.* 10^{-3} M in complex. [c] Anodic peak potential for an irreversible process. [d] Quasi-reversible wave (ΔE_p > 120 mV). [e] 2-min irradiation with a 150-W Reflector Spot lamp.

Table II. Crystallographic Data and Refinement Details for *trans*-$[Ru(bpy)_2(4\text{-Etpy})(DMSO)](PF_6)_2\cdot 0.5DMF$

empirical formula	$C_{30.5}H_{34.5}F_{12}N_{5.5}O_{1.5}P_2RuS$
fw	925.19
space group	$P2_1/c$
a, Å	15.0301(9)
b, Å	18.1948(12)
c, Å	14.6323(7)
β, deg	97.769(5)
V, Å^3	3964.8(4)
Z	4
D_{calc}, Mg m^{-3}	1.550
T, K	298
λ(Mo Kα), Å	0.710 73
F(000)	1860.57
μ, mm^{-1}	0.60
scan type	$\theta/2\theta$
2θ limit, deg	45
h,*k*,*l* ranges	$\bar{1}5$–16,0–19,0–15
tot. no. of reflns	5152
no. of unique reflns	5152
no. of data with $I > 2.5\sigma(I)$	3461
R^a	0.065
$R_w{}^a$	0.084
GOF	2.31
no. of params	612
max residual electron density, e/Å^3	1.14
min residual electron density, e/Å^3	–0.48

[a] $R = \sum(|F_o| - |F_c|)/\sum|F_o|$; $R_w = [\sum w(F_o - F_c)^2/\sum wF_o^2]^{1/2}$; GOF = $[\sum w(F_o - F_c)^2/(\text{no. of reflns} - \text{no. of params})]^{1/2}$.

Table III. Selected Bond Distances (Å) for *trans*-$[Ru(bpy)_2(4\text{-Etpy})(DMSO)](PF_6)_2\cdot 0.5DMF$

Ru(1)–S(1)	2.257(3)	Ru(1)–N(42)	2.103(7)
Ru(1)–N(11)	2.108(8)	Ru(1)–N(51)	2.147(8)
Ru(1)–N(22)	2.105(7)	S(1)–O(1)	1.479(1)
Ru(1)–N(31)	2.081(7)	S(1)–C(2)	1.781(11)
Ru(1)–C(36)	2.896(10)	S(1)–C(3)	1.769(11)
Ru(1)–C(37)	2.872(9)		

isomerization to the cis form is observed over extended periods if the reaction is kept in the dark. This contrasts with the observation of isomerization at room temperature in the dark for *trans*-$[Ru(bpy)_2(H_2O)_2](CF_3SO_3)_2$ in aqueous acidic solution.[14] **1** reacts readily with the pyridyl ligands 4-ethylpyridine (4-Etpy), 4-(dimethylamino)pyridine (DMAP), and ethyl isonicotinate (ISNE) at room temperature in DMSO solution to form the salts *trans*-$[Ru(bpy)_2(py)(DMSO)](PF_6)_2\cdot nH_2O$ (py = 4-Etpy, *n* = 0 (**2**); py = DMAP, *n* = 1.5 (**3**); py = ISNE, *n* = 1 (**4**)). It has been found that when a stoichiometric amount of pyridyl ligand is used, unreacted **1** persists after several days, but if a large excess of pyridyl ligand is added, all of the bis(dimethyl sulfoxide) complex is consumed after a period of 15 h. Again, no isomerization occurs if the reaction is left for extended periods in the dark.

(14) Durham, B.; Wilson, S. R.; Hodgson, D. J.; Meyer, T. J. *J. Am. Chem. Soc.* **1980**, *102*, 600.

Table IV. Selected Bond Angles (deg) for *trans*-$[Ru(bpy)_2(4\text{-Etpy})(DMSO)](PF_6)_2\cdot 0.5DMF$

S(1)–Ru(1)–N(11)	95.38(22)	C(37)–Ru(1)–N(42)	25.3(3)
S(1)–Ru(1)–N(22)	87.77(22)	C(37)–Ru(1)–N(51)	73.1(3)
S(1)–Ru(1)–N(31)	90.06(22)	N(42)–Ru(1)–N(51)	85.8(3)
S(1)–Ru(1)–C(36)	103.27(20)	Ru(1)–S(1)–O(1)	112.9(3)
S(1)–Ru(1)–C(37)	107.16(20)	Ru(1)–S(1)–C(2)	115.5(4)
S(1)–Ru(1)–N(42)	96.50(22)	Ru(1)–S(1)–C(3)	113.9(4)
S(1)–Ru(1)–N(51)	174.79(22)	O(1)–S(1)–C(2)	106.5(5)
N(11)–Ru(1)–N(22)	76.6(3)	O(1)–S(1)–C(3)	106.3(5)
N(11)–Ru(1)–N(31)	174.6(3)	C(2)–S(1)–C(3)	100.6(6)
N(11)–Ru(1)–C(36)	151.6(3)	Ru(1)–N(11)–C(12)	127.1(7)
N(11)–Ru(1)–C(37)	123.7(3)	Ru(1)–N(11)–C(16)	116.3(6)
N(11)–Ru(1)–N(42)	103.5(3)	Ru(1)–N(22)–C(17)	116.4(6)
N(11)–Ru(1)–N(51)	88.6(3)	Ru(1)–N(22)–C(21)	125.6(7)
N(22)–Ru(1)–N(31)	103.6(3)	Ru(1)–N(31)–C(32)	128.9(6)
N(22)–Ru(1)–C(36)	124.8(3)	Ru(1)–N(31)–C(36)	113.7(6)
N(22)–Ru(1)–C(37)	152.1(3)	Ru(1)–C(36)–N(31)	41.2(4)
N(22)–Ru(1)–N(42)	175.7(3)	Ru(1)–C(36)–C(35)	160.0(8)
N(22)–Ru(1)–N(51)	89.9(3)	Ru(1)–C(36)–C(37)	74.2(5)
N(31)–Ru(1)–C(36)	25.2(3)	Ru(1)–C(37)–C(36)	76.0(5)
N(31)–Ru(1)–C(37)	54.3(3)	Ru(1)–C(37)–C(38)	159.9(7)
N(31)–Ru(1)–N(42)	75.9(3)	Ru(1)–C(37)–N(42)	42.8(4)
N(31)–Ru(1)–N(51)	85.9(3)	Ru(1)–N(42)–C(37)	112.0(6)
C(36)–Ru(1)–C(37)	29.9(3)	Ru(1)–N(42)–C(41)	127.7(6)
C(36)–Ru(1)–N(42)	53.7(3)	Ru(1)–N(51)–C(52)	121.6(6)
C(36)–Ru(1)–N(51)	74.3(3)	Ru(1)–N(51)–C(56)	122.1(7)

A crystal structure determination on *trans*-$[Ru(bpy)_2(4\text{-Etpy})(DMSO)](PF_6)_2$ (**2**) (*vide infra*) reveals that the second DMSO ligand is S-bound. This is in keeping with the crystallographically established preference of Ru(II) for binding via the sulfur atom of DMSO[15] and implies a relatively strong Ru–S bond. In accordance with this observation, it has been found that substitution of the second DMSO ligand in **2** is accomplished much less readily than the initial replacement. ^1H NMR experiments have revealed that no reaction occurs in solutions of

(15) (a) March, F. C.; Ferguson, G. *Can. J. Chem.* **1971**, *49*, 3590. (b) McMillan, R. S.; Mercer, A.; James, B. R.; Trotter, J. *J. Chem. Soc., Dalton Trans.* **1975**, 1006. (c) Mercer, A.; Trotter, J. *J. Chem. Soc., Dalton Trans.* **1975**, 2480. (d) Davies, A. R.; Einstein, F. W. B.; Farrell, N. P.; James, B. R.; McMillan, R. S. *Inorg. Chem.* **1978**, *17*, 1965. (e) Oliver, J. D.; Riley, D. P. *Inorg. Chem.* **1984**, *23*, 156.

Table V. Final Atomic Fractional Coordinates and Equivalent Isotropic Displacement Coefficients (Å²) for *trans*-[Ru(bpy)₂(4-Etpy)(DMSO)](PF₆)₂·0.5DMF

atom	x	y	z	B_{iso}[a]
Ru(1)	0.29575(5)	0.52521(5)	0.12817(5)	2.97(3)
S(1)	0.37174(17)	0.61783(14)	0.07135(17)	3.44(12)
O(1)	0.4457(5)	0.5918(4)	0.0225(5)	4.6(4)
C(2)	0.3058(8)	0.6786(6)	-0.0056(8)	4.9(6)
C(3)	0.4202(8)	0.6806(6)	0.1561(8)	5.3(6)
N(11)	0.1682(5)	0.5591(4)	0.0643(5)	3.5(4)
C(12)	0.1058(7)	0.5957(6)	0.1034(7)	4.1(5)
C(13)	0.0248(7)	0.6172(6)	0.0568(8)	4.9(6)
C(14)	0.0046(7)	0.6017(7)	-0.0337(8)	5.4(6)
C(15)	0.0666(7)	0.5629(6)	-0.0741(7)	4.8(6)
C(16)	0.1467(7)	0.5412(5)	-0.0271(7)	3.6(5)
C(17)	0.2150(7)	0.4968(5)	-0.0642(7)	3.5(4)
C(18)	0.2078(7)	0.4768(7)	-0.1560(7)	4.7(6)
C(19)	0.2707(7)	0.4321(7)	-0.1862(7)	5.2(6)
C(20)	0.3411(7)	0.4087(7)	-0.1248(8)	5.2(6)
C(21)	0.3475(7)	0.4306(6)	-0.0333(7)	4.2(5)
N(22)	0.2851(5)	0.4760(5)	-0.0031(5)	3.5(4)
N(31)	0.4156(5)	0.4834(4)	0.1963(5)	3.1(3)
C(32)	0.4870(6)	0.4570(6)	0.1604(7)	3.9(5)
C(33)	0.5535(7)	0.4153(7)	0.2086(8)	5.4(6)
C(34)	0.5501(8)	0.4043(7)	0.3034(9)	5.8(6)
C(35)	0.4805(8)	0.4353(6)	0.3431(7)	4.9(6)
C(36)	0.4166(6)	0.4772(6)	0.2881(7)	3.8(5)
C(37)	0.3476(6)	0.5233(6)	0.3244(6)	3.4(4)
C(38)	0.3407(7)	0.5271(7)	0.4201(7)	4.8(6)
C(39)	0.2852(8)	0.5833(8)	0.4483(8)	6.3(7)
C(40)	0.2444(7)	0.6312(7)	0.3832(8)	5.2(6)
C(41)	0.2541(7)	0.6235(6)	0.2923(7)	4.1(5)
N(42)	0.3022(5)	0.5671(4)	0.2629(5)	3.2(4)
N(51)	0.2333(5)	0.4306(5)	0.1801(5)	3.8(4)
C(52)	0.2668(7)	0.3632(6)	0.1736(8)	4.7(6)
C(53)	0.2366(8)	0.3032(6)	0.2134(8)	5.3(6)
C(54)	0.1643(7)	0.3104(6)	0.2655(7)	4.6(5)
C(55)	0.1309(7)	0.3797(6)	0.2718(7)	4.2(5)
C(56)	0.1642(6)	0.4365(6)	0.2295(7)	3.8(5)
C(57)	0.1349(8)	0.2449(7)	0.3200(9)	5.7(6)
C(58)	0.1873(9)	0.2385(8)	0.4127(10)	7.4(8)
O(61)	-0.0142(8)	0.0582(7)	0.2187(8)	3.6(3)
C(62)	0.0079(21)	0.0528(17)	0.1812(21)	8.5(8)
N(63)	0.0505(10)	0.0984(9)	0.1002(11)	3.6(3)
C(64)	0.0265(16)	0.1641(13)	0.0975(17)	5.7(6)
C(65)	0.1051(22)	0.0698(18)	0.0456(23)	9.2(9)
P(1)	0.16244(21)	0.82862(18)	0.18464(23)	5.34(16)
F(11)	0.21823(21)	0.90377(18)	0.18398(23)	20.4(29)
F(12)	0.14224(21)	0.83311(18)	0.07536(23)	13.2(17)
F(13)	0.10866(21)	0.75555(18)	0.18405(23)	20.6(28)
F(14)	0.18465(21)	0.82621(18)	0.29267(23)	16.7(22)
F(15)	0.07509(21)	0.87479(18)	0.19238(23)	7.5(9)
F(16)	0.25179(21)	0.78453(18)	0.17565(23)	9.7(12)
F(31)	0.24679(21)	0.80519(18)	0.25303(23)	12.7(12)
F(32)	0.11824(21)	0.86351(18)	0.26589(23)	19.1(20)
F(33)	0.07786(21)	0.85379(18)	0.11371(23)	17.5(16)
F(34)	0.20641(21)	0.79547(18)	0.10085(23)	17.0(17)
F(35)	0.11565(21)	0.75338(18)	0.19801(23)	13.7(14)
F(36)	0.20900(21)	0.90560(18)	0.16873(23)	13.4(13)
P(2)	0.4298(3)	0.18515(21)	0.0833(3)	7.44(22)
F(21)	0.4577(3)	0.20131(21)	-0.0160(3)	12.6(13)
F(22)	0.5278(3)	0.20800(21)	0.1285(3)	14.9(16)
F(23)	0.4035(3)	0.16850(21)	0.1813(3)	10.7(12)
F(24)	0.3334(3)	0.16181(21)	0.0368(3)	16.2(15)
F(25)	0.4633(3)	0.10282(21)	0.0758(3)	16.5(17)
F(26)	0.3978(3)	0.26699(21)	0.0895(3)	20.1(21)
F(41)	0.3345(3)	0.16880(21)	0.1161(3)	15.6(19)
F(42)	0.3931(3)	0.14951(21)	-0.0143(3)	19.8(26)
F(43)	0.5222(3)	0.20022(21)	0.0493(3)	17.9(25)
F(44)	0.4636(3)	0.21951(21)	0.1797(3)	29.8(41)
F(45)	0.4631(3)	0.10661(21)	0.1195(3)	21.1(27)
F(46)	0.3936(3)	0.26241(21)	0.0459(3)	8.8(11)

[a] B_{iso} is the mean of the principal axes of the thermal ellipsoid.

pyridine or acetonitrile at room temperature in the dark over several days. If the solutions are exposed to light, reaction accompanied by isomerization takes place. Thermal displacement of the DMSO by a pyridyl ligand can be accomplished at temperatures above *ca.* 80 °C, but unless a large excess of ligand is present, isomerization occurs. Furthermore, the use of excess of a second pyridyl ligand gives rise to replacement not only of the DMSO but also of the 4-Etpy ligand. This can yield mixtures containing up to 50% of the symmetrical bis(pyridine) complex. The sensitive nature of these trans complexes coupled with their generally poor solubility characteristics effectively preclude the use of chromatographic techniques to separate such mixtures.

Since it has been established that neither thermal nor photochemical substitution by pyridyl ligands provides routes to the desired asymmetric trans complexes, attention was turned to chemical methods of replacing the DMSO ligand. Hopes that the DMSO might be labilized by oxidation to dimethyl sulfone[16] have been proven ill-founded by electrochemical studies (*vide infra*). Also, a report describing the base-catalyzed labilization of S-bound DMSO in Ru(II) complexes[17] is very likely to be simply an observation of H/D exchange of the acidic methyl protons. Of considerable interest is an account of acid-catalyzed aquation in the complex $[Ru(trpy)(bpy)(DMSO)]^{2+}$ (trpy = 2,2′:6,2″-terpyridine).[18] However, it has been found that **2** is inert toward concentrated HCl in methanol unless heated to *ca.* 80 °C. The yellow product from this reaction has been identified as *trans*-$[Ru(bpy)_2(DMSO)Cl]PF_6$ on the basis of ^1H NMR and UV–vis spectroscopy.[19] This demonstrates that the DMSO ligand in **2** is unusually stable to acid attack and rules out any potential for acid-catalyzed substitution.

As described earlier, thermal replacement of the DMSO in **2** by a pyridyl ligand is accompanied by a large degree of exchange of the 4-Etpy ligand. It is likely that this occurs prior to substitution of DMSO owing to the moderately high trans-labilizing influence of S-bound DMSO.[20] However, the observation that extended reaction times result in increasing degrees of 4-Etpy exchange shows that the trans-labilizing effect of a pyridyl ligand in these systems is also significant. When **2** is heated with excess KCN or $NaNO_2$ in DMSO, the strong trans-labilizing effects of the π-acceptor ligands CN^- and NO_2^- result in almost quantitative formation of the complexes *trans*-$Ru(bpy)_2(CN)_2$ and *trans*-$Ru(bpy)_2(NO_2)_2$, respectively. These compounds are totally insoluble in all common solvents and have been characterized by IR spectroscopy and elemental analyses.[21] They are more readily prepared in quantitative yield from the salt *trans*-$[Ru(bpy)_2(H_2O)_2](CF_3SO_3)_2$.[22]

When **2** is heated with an excess of LiCl, the major product is *trans*-$[Ru(bpy)_2(4\text{-}Etpy)Cl]PF_6 \cdot H_2O$ (**5**). If the reaction is carried out in a saturated solution of LiCl in aqueous DMF, then some precipitation of this product occurs even at 105 °C. The complete lack of solubility of **5** in water facilitates its isolation in pure form, but yields of *ca.* 65% demonstrate that a large proportion of the starting complex in **2** is not converted to the desired product. The addition of aqueous NH_4PF_6 to the golden filtrate obtained after removal of the product **5** affords a yellow solid identified as the same compound, *trans*-$[Ru(bpy)_2(DMSO)Cl]PF_6$, isolated when **2** is heated with concentrated HCl.[19] Of particular interest is the observation that not even a trace of the totally insoluble *trans*-$Ru(bpy)_2Cl_2$ is produced in this reaction.

(16) Roecker, L.; Dobson, J. C.; Vining, W. J.; Meyer, T. J. *Inorg. Chem.* **1987**, *26*, 779.
(17) Farrel, N.; De Oliveira, N. G. *Inorg. Chim. Acta* **1980**, *44*, L255.
(18) Root, M. J.; Deutsch, E. *Inorg. Chem.* **1985**, *24*, 1464.
(19) δ_H (CD_3SOCD_3) 9.32 (4 H, d, J = 5.4 Hz, *bpy* × 2), 8.71 (4 H, d, J = 7.7 Hz, *bpy* × 2), 8.27 (4 H, t, J = 7.5 Hz, *bpy* × 2), 7.78 (4 H, t, J = 6.3 Hz, *bpy* × 2), 2.44 (6 H, s, *Me*₂SO); λ_{max}(DMSO) 296, 438 nm.
(20) (a) Kukushkin, Y. N. *Inorg. Chim. Acta* **1974**, *9*, 117. (b) Elding, L. I.; Grönning, O. *Inorg. Chem.* **1978**, *17*, 1872.
(21) The complex *trans*-$Ru(bpy)_2(CN)_2$ was isolated as a dark red-purple solid. ν(CN) 2062 cm⁻¹. Anal. Calcd for $C_{22}H_{16}N_6Ru \cdot H_2O$: C, 54.65; H, 3.75; N, 17.38. Found: C, 54.60; H, 3.42; N, 17.16. The complex *trans*-$Ru(bpy)_2(NO_2)_2$ was isolated as a red solid. Anal. Calcd for $C_{20}H_{16}N_6O_4Ru$: C, 47.53; H, 3.19; N, 16.63. Found: C, 47.30; H, 3.15; N, 16.46.
(22) Coe, B. J.; Thompson, D. W. Unpublished results.

Scheme I. Preparation of *trans*-Bis(2,2′-bipyridine)ruthenium Complexes (Etpy = 4-Ethylpyridine)

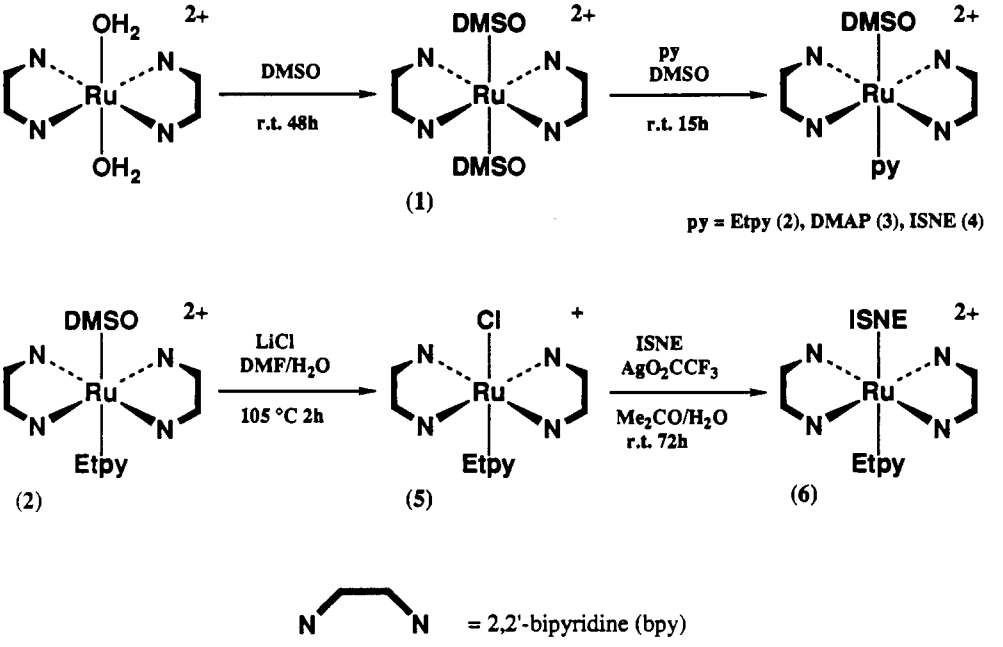

This demonstrates that Cl^- does not exert a trans-labilizing effect either on the 4-Etpy ligand or on DMSO, since reaction of either **5** or *trans*-$[Ru(bpy)_2(DMSO)Cl]PF_6$ with another Cl^- ion would yield *trans*-$Ru(bpy)_2Cl_2$.

The chloride ligand in **5** is sufficiently labile to enable abstraction by silver(I) trifluoroacetate at ambient temperature. If this reaction is carried out in pure acetone with excess ISNE, precipitation of AgCl is observed and a dark purple solid isolated. This material has a UV–visible spectrum almost identical in absorption profile to that of **5**, but with blue shifts in the maxima of 10–20 nm.[23] This suggests the formation of the salt *trans*-$[Ru(bpy)_2(4\text{-Etpy})(CF_3CO_2)]PF_6$, which does not react further with ISNE in acetone. However, if the abstraction is carried out in aqueous acetone, then an excellent yield of the mixed pyridine salt *trans*-$[Ru(bpy)_2(4\text{-Etpy})(ISNE)](PF_6)_2$ (**6**) is obtained. Hence it appears that a relatively strongly coordinating solvent such as water must be present in order to facilitate substitution of the anionic $CF_3CO_2^-$ ligand by the neutral ISNE. The reactiion sequence leading to **6** is shown in Scheme I. The overall yield of **6** prepared in four steps starting from *trans*-$[Ru(bpy)_2(H_2O)_2](CF_3SO_3)_2$ is 61%.

^{1}H NMR Studies. Complexes of the form *trans*-$[Ru(bpy)_2(X)(Y)]^{n+}$ have well-defined ^{1}H NMR spectra, which aid greatly in their identification. In particular, the bpy protons of the *trans*-$[Ru(bpy)_2]^{2+}$ fragment give a diagnostic pattern of doublet, doublet, triplet, triplet (in order of increasing field strength) with integrals 4:4:4:4 in the range 9.8–7.7 ppm in DMSO-d_6 solution. The precise chemical shifts of these multiplets are determined by the electronic properties of the Ru center, and hence by the axial ligands. The lowest field bpy doublet is found to be the most sensitive indicator and can vary over a range of about 0.4 ppm, whereas the other three multiplets only vary over *ca.* 0.15–0.10 ppm. All of the new complexes reported show this characteristic pattern together with signals assigned to the axial ligands.

Of particular interest to this study are the resonances observed for coordinated DMSO molecules. Previous reports have assigned signals occurring *ca.* 1 ppm downfield of free DMSO (at 2.53 ppm in DMSO-d_6) to S-bound DMSO, while O-bound DMSO has been found to give signals very close to those of free DMSO.[15b,d,24] For **1** the spectrum in weakly coordinating methanol-d_4 shows two singlets at 2.65 and 2.62 ppm of integral 6:6 which are invariant with time. The lower field resonance corresponds to free DMSO. This suggests that one of the DMSO ligands in **1** is rapidly replaced by methanol, but once this exchange has occurred, the second DMSO is not labile at room temperature. It seems likely that the remaining DMSO is S-bound since the occurrence of O-bound DMSO with Ru(II) has only previously been reported in cases where it exists trans to an S-bound DMSO.[15c,d] This is believed to be because of an electronic stabilization from O-bound DMSO functioning as a strong σ-donor and the S-bound as a π-acceptor.[15d]

When the spectrum of **1** is recorded in DMSO-d_6, a rather different pattern is observed. At 10 min after dissolution, three signals are observed at 2.60, 2.34, and 1.94 ppm of relative intensity 3:1:2, and a singlet is observed for free DMSO of integral 6, which accounts for 50% of the total originally coordinated. After 60 min at ambient temperature, all three signals assigned to bound DMSO completely vanish and the free DMSO singlet integrates for 12 protons, indicating complete exchange of the initially bound DMSO by DMSO-d_6. Furthermore the bpy region shows small overlapping "shadow" multiplets for all but the higher field doublet, and this pattern remains unchanged with time.

It is not possible with the data available to rationalize this behavior conclusively, but it seems that the complex of **1** in DMSO solution exists as a mixture of the possible S- and O-bound isomers. The most stable isomers are likely to be the S/S-bound and S/O-bound forms, with the O/O-bound being unlikely. The observation of a major and a minor set of bpy multiplets supports this hypothesis. Exchange of the bound DMSO is clearly rapid, and this may be a result of loss of either S- or O-bound DMSO. However, it is perhaps reasonable to suggest that S-bound DMSO converts to O-bound before exchange can occur. Facile exchanges of both S- and O-bound DMSO have been previously reported for several other Ru(II)–DMSO complexes,[15b,d,24b] with slower exchange observed for S-bound compared to O-bound molecules.

All of the salts **2**–**4** show only single resonances for bound DMSO which do not exhibit any tendency for exchange at room temperature in the dark. These signals all occur in the narrow range 2.60–2.57 ppm, which is only 0.07–0.04 ppm downfield of

(23) λ_{max}(DMSO) 302, 360, 506 nm.

(24) (a) Senoff, C. V.; Maslowsky, E.; Goel, R. G. *Can. J. Chem.* **1971**, *49*, 3585. (b) Evans, I. P.; Spencer, A.; Wilkinson, G. *J. Chem. Soc., Dalton Trans.* **1973**, 204.

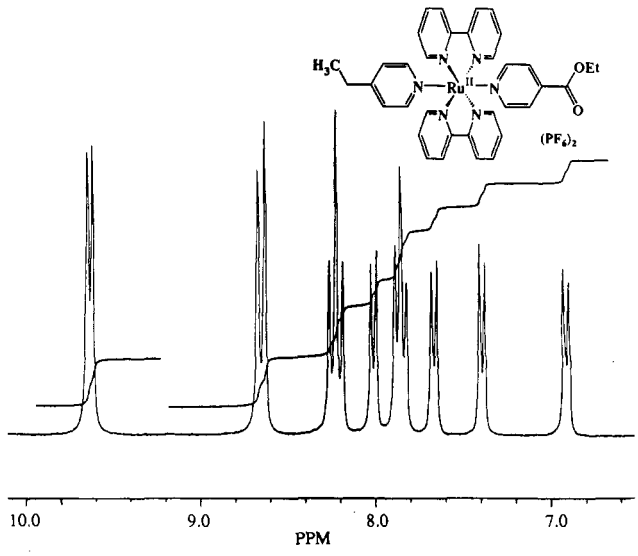

Figure 1. Aromatic region of the ^1H NMR spectrum of *trans*-[$Ru(bpy)_2$(4-Etpy)(ISNE)]$(PF_6)_2$ (**6**) in DMSO-d_6 vs TMS.

the free-DMSO signal. Since the DMSO is known to be S-bound, at least in **2**, these values demonstrate a much smaller degree of deshielding of the methyl protons when compared to values for other Ru(II)–DMSO complexes. This is likely to be a result of the counterbalancing shielding effect of the ring currents due to the bpy ligands. Similarly high-field signals assigned to S-bound DMSO have previously been observed in Ru(II)–DMSO complexes of a tetrapyrazolic macrocycle.[10]

The axial pyridyl ligands give rise to characteristic AA'BB' splitting patterns together with signals for the methyl and ethyl substituents. The positions of the AA'BB' signals are found to vary greatly with the nature of the 4-substituent, with **4** showing the lowest field resonances due to the deshielding effect of the $-CO_2Et$ group. The shielding effect of the $-NMe_2$ group gives rise to a relatively high-field AA'BB' pattern for **3**, the center of which is *ca.* 1.2 ppm upfield of that for **4**. The judicious choice of the ligands 4-Etpy and ISNE results in a spectrum for **6** in which all of the aryl multiplets are clearly resolved (Figure 1). Hence the ^1H NMR spectrum serves as an especially powerful tool in the identification of this complex. Small but significant shifts for the AA'BB' and Et multiplets of the 4-Etpy ligand are observed for the *trans*-$[Ru(bpy)_2(4\text{-Etpy})(Y)]^{n+}$ complexes **2** (Y = DMSO, n = 2), **5** (Y = Cl, n = 1), and **6** (Y = ISNE, n = 2) due to the trans effect of the Y ligand.

Infrared Studies. Spectra were recorded for all of the new salts primarily in order to assign the SO stretching vibrations of the bound DMSO molecules. Previous reports have shown that S-bound DMSO gives bands around 1100 cm^{-1}, which is to high frequency of that of free DMSO (*ca.* 1055 cm^{-1}).[15b] This is attributed to an increase in the SO bond order, implying that the electron density donated from S to Ru is of an antibonding nature with respect to the SO bond. Conversely, O-bound DMSO leads to a lower vibrational frequency of *ca.* 915 cm^{-1}, owing to a decrease in the SO bond order resulting from extensive σ-donation from O to Ru. Unfortunately, the complex nature of the spectra obtained for salts **1**–**6** renders impossible any conclusive identification of bands due to bound DMSO, but data are reported for the sake of completeness.[25]

UV–Visible Studies. Electronic spectra for the new complexes were recorded in DMSO solution, and data are presented in Table I. The DMSO-containing salts **1**–**4** are all yellow and exhibit a single intermediate-intensity MLCT band at the violet end of the visible spectrum together with a single high-intensity π–π^* band in the UV. The energy of the MLCT band is found to vary to some degree with the nature of X in *trans*-$[Ru(bpy)_2(X)(DMSO)]^{2+}$, but only a very small blue shift is observed when X = DMSO (**1**) is replaced with 4-Etpy (**2**). Similar behavior has been reported for the previously described Ru(II)–DMSO complexes of a tetrapyrazolic macrocycle.[10] The electronic influence of the 4-pyridyl substituent R in *trans*-$[Ru(bpy)_2(py\text{-}R)(DMSO)](PF_6)_2$ can be seen in the blue shift of 6 nm going from R = Et (**2**) to R = CO_2Et (electron-withdrawing, **4**). A much larger red shift of 18 nm is produced when the ethyl group in **2** is replaced by the strongly electron-donating NMe_2 group (in **3**). The energies of the π–π^* bands are found to be almost invariant in this group of complexes.

The purple-red salt **5** has an absorption profile which is very different from those of the DMSO complexes. In this case, one high-intensity and two medium-intensity UV bands are observed together with two bands in the green region of the visible spectrum. The orange salt **6** has two high-intensity and one medium-intensity UV bands, and the MLCT band occurs in the blue region. The striking changes in visible absorption characteristics for the series of 4-Etpy complexes in the salts **2**, **5**, and **6** serve to facilitate greatly the spectrophotometric monitoring of the reaction sequence leading to **6**.

Electrochemical Studies. The oxidative electrochemical properties of the new complexes were investigated by cyclic voltammetry in acetonitrile solution in the dark. Results are presented in Table I. The DMSO-containing complexes in salts **1**–**4** all show similar behavior. No redox events are observed on cycling between 0 and 1 V, but if the range is extended to 2 V, an initial completely irreversible oxidation is observed in the region 1.83–1.47 V. The position of this wave depends on the nature of X in *trans*-$[Ru(bpy)_2(X)(DMSO)]^{2+}$, with an anodic shift of 150 mV produced by replacing X = DMSO (**1**) with 4-Etpy (**2**). The electronic influence of the 4-pyridyl substituent R in *trans*-$[Ru(bpy)_2(py\text{-}R)(DMSO)](PF_6)_2$ can be seen in the anodic shift of 60 mV on going from R = Et (**2**) to R = CO_2Et (**4**). A much larger cathodic shift of 300 mV is produced when the ethyl group in **2** is replaced by the strongly electron-donating NMe_2 group (in **3**), and oxidation becomes considerably more favorable. These changes are in qualitative agreement with those observed in the electronic absorption spectra.

Once the irreversible oxidation has occurred, further waves are generated in the region 0.69–1.41 V. For **1**, **2**, and **4**, two reversible waves are observed. These waves as well as the initial oxidation wave are stable to repeated cycling. Again, the positions of the two product waves depend on the electronic properties of X in *trans*-$[Ru(bpy)_2(X)(DMSO)]^{2+}$. They are most anodic for X = ISNE (**4**) and least anodic for X = DMSO (**1**), with intermediate potentials for X = 4-Etpy (**2**). The cathodic shifts for the most anodic wave are 80 mV on going from X = ISNE to X = 4-Etpy and 240 mV on going from X = 4-Etpy to X = DMSO. Those for the least anodic wave are 80 mV on going from X = ISNE to X = 4-Etpy and 300 mV on going from X = 4-Etpy to X = DMSO. For **3**, only a single reversible product wave is found at 0.78 V. Both this wave and the initial oxidation wave are also stable to repeated cycling.

Clearly, oxidation of these complexes brings about a reaction in which the X ligand is retained, but a change occurs at the DMSO ligand. By marked contrast, reversible Ru(III/II) waves were reported for the complexes $[Ru(TZ)(DMSO)_2]^{2+}$ and $[Ru(TZ)(py)(DMSO)]^{2+}$ (TZ = 2,7,12,17-tetramethyl-1,6,11,16-tetraazaporphyrinogen, py = pyridine).[10] Previous workers have described S to O linkage isomerization upon oxidation of Ru(II)

(25) Infrared data: For **1** four bands that are possibly SO in origin are observed at 1149 (s), 1098 (m), 1034 (s), and 939 (w) cm^{-1}, while metathesis to *trans*-$[Ru(bpy)_2(DMSO)_2](PF_6)_2$ gives only three bands at 1113 (s), 1011 (s), and 912 (m) cm^{-1}. The fully deuterated complex *trans*-$[Ru(bpy)_2(DMSO\text{-}d_6)_2](CF_3SO_3)_2$ has bands at 1150 (s), 1099 (m), 1031 (s), and 939 (w) cm^{-1}, which show negligible shifts from those of **1**. Five bands are found for **2** at 1101 (m), 1056 (m), 1034 (m), 1012 (m), and 912 (w) cm^{-1}, while **3** has vibrations at 1096 (m), 1063 (w), and 1018 (m) cm^{-1}, and a total of eight bands are observed in the region 1150–900 cm^{-1} for **4**.

Scheme II. Suggested Reaction Sequence Following Electrochemical Oxidation of a Complex of the Type *trans*-$[Ru(bpy)_2(DMSO)(X)]^{2+}$ (X = DMSO, 4-Etpy, ISNE, DMAP)

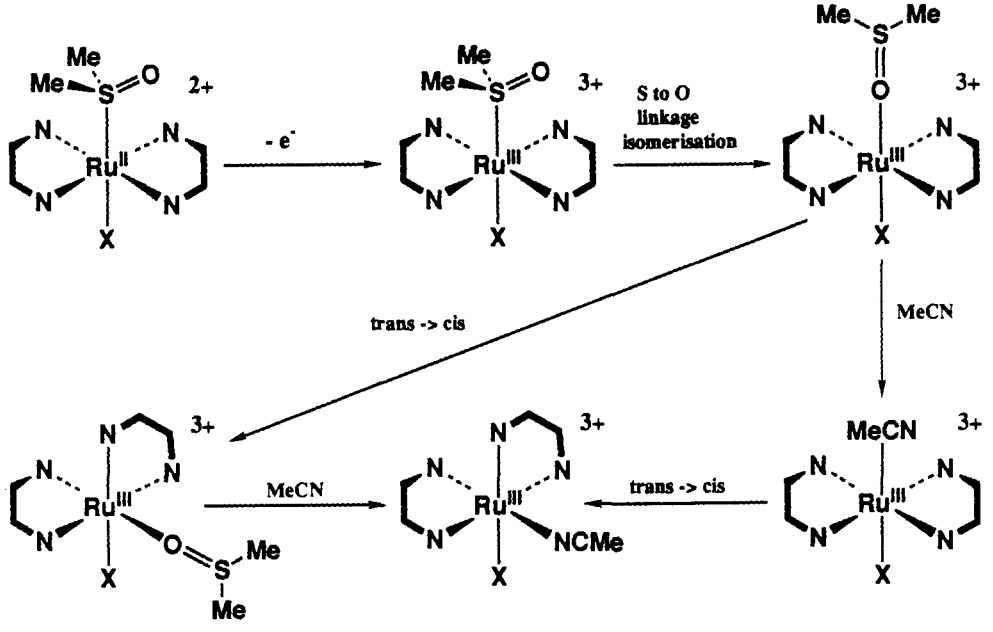

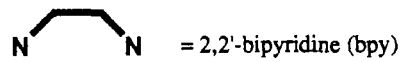

to Ru(III) in the complex $[Ru(NH_3)_5(DMSO)]^{2+}$ which is reversed upon reduction back to Ru(II).[26] The change from the S- to the O-bound form causes a cathodic shift of 1 V in the M(III/II) reduction potential. It is suggested that this is occurring in the present case, but this possibility alone does not explain the appearance of two new waves for **1**, **2**, or **4**. Also likely is that solvolysis by acetonitrile is taking place perhaps accompanied by isomerization to the cis form. It has been observed previously that trans to cis isomerization in the complexes $[Ru(bpy)_2(X)_2]^{2+}$ (X = pyridine, acetonitrile) does not lead to a marked change in the potential of the M(III/II) couple.[5] Therefore, the most likely products of oxidation may be *trans*- or *cis*-$[Ru(bpy)_2(X)(Y)]^{2+}$ (where X = DMSO, 4-Etpy, ISNE, DMAP; Y = O-bound DMSO or MeCN), and even if all four are produced, it is possible that only two waves will be observed. Quite why only a single product is observed for **3** is unclear. A suggested reaction sequence to explain the electrochemical behavior is given in Scheme II.

The oxidative behavior of the remaining two complexes in salts **5** and **6** is much more straightforward. For **6**, a reversible oxidation wave is observed at 1.29 V, which is the same potential as that previously reported for *trans*-$[Ru(bpy)_2(py)_2](ClO_4)_2$.[5] No new waves are generated by repeated cycling. In the case of **5**, a reversible oxidation wave is found at the considerably more cathodic potential of 0.72 V. The complex *cis*-$[Ru(bpy)_2(py)Cl]^+$ has a reduction potential of 0.79 V vs SCE in acetonitrile.[27]

Exposure of the complex/electrolyte solutions to a 150-W Reflector Spot lamp accompanied by oxidative cycling yields some information concerning the photolytic behavior of these complexes. Data are shown in Table I. In all cases, complete loss of the oxidation waves observed in the dark is accompanied by the growth of a single reversible or quasi-reversible (ΔE_p > 120 mV) product wave. All but two of these products undergo oxidation at differing potentials, and they are all stable to ambient light for at least 24 h. For **1** and **4**, the product potentials are very close to those previously reported for *cis*- and *trans*-$[Ru(bpy)_2(MeCN)_2](ClO_4)_2$.[5] However, it is unlikely that solvolysis of both axial ligands is occurring, since this is clearly not the case for the other complexes. More likely is the suggestion that **1**, **3**, and **4** are photolyzed to *cis*-$[Ru(bpy)_2(X)(MeCN)]^{2+}$ (X = DMSO, DMAP, and ISNE, respectively), while **2** and **6** are both converted to *cis*-$[Ru(bpy)_2(4\text{-Etpy})(MeCN)]^{2+}$ and **5** gives *cis*-$[Ru(bpy)_2(MeCN)Cl]^+$.

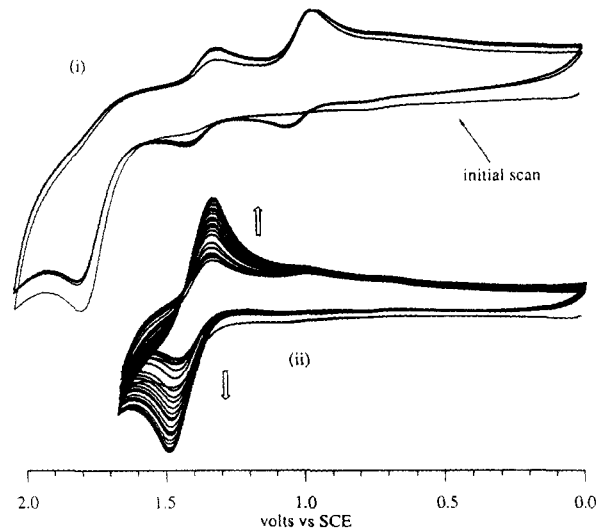

Figure 2. Cyclic voltammograms for **2**, *trans*-$[Ru(bpy)_2(4\text{-Etpy})(DMSO)](PF_6)_2$, in 0.1 M $[N(C_4H_9\text{-}n)_4][PF_6]$ at 200 mV s^{-1} (*Y* sensitivity = 10 mV cm^{-1}): (i) 0.0–2.0 V, five scans; (ii) 0.0–1.65 V, repetitive cycling with continuous irradiation by a 150-W Reflector Spot lamp showing growth of photolysis product wave.

These suggestions are strongly supported by comparison with the published reduction potentials in acetonitrile of 1.35 V vs SCE for *cis*-$[Ru(bpy)_2(py)(MeCN)]^{2+}$ [27] and 0.86 V vs SSCE for *cis*-$[Ru(bpy)_2(MeCN)Cl]^+$.[3d] Further preparative-scale experiments are required in order to achieve a better understanding of these reactions and of those induced by electrochemical oxidation. Representative cyclic voltammograms for **2** illustrating both oxidative behavior in the dark and the effect of photolysis are shown in Figure 2.

X-ray Crystal Structure of 2. Figure 3a shows one view of the X-ray structure of the cation *trans*-$[Ru(bpy)_2(4\text{-Etpy})(DM-$

(26) Yeh, A.; Scott, N.; Taube, H. *Inorg. Chem.* **1982**, *21*, 2542.
(27) Sullivan, B. P.; Conrad, D.; Meyer, T. J. *Inorg. Chem.* **1985**, *24*, 3640.

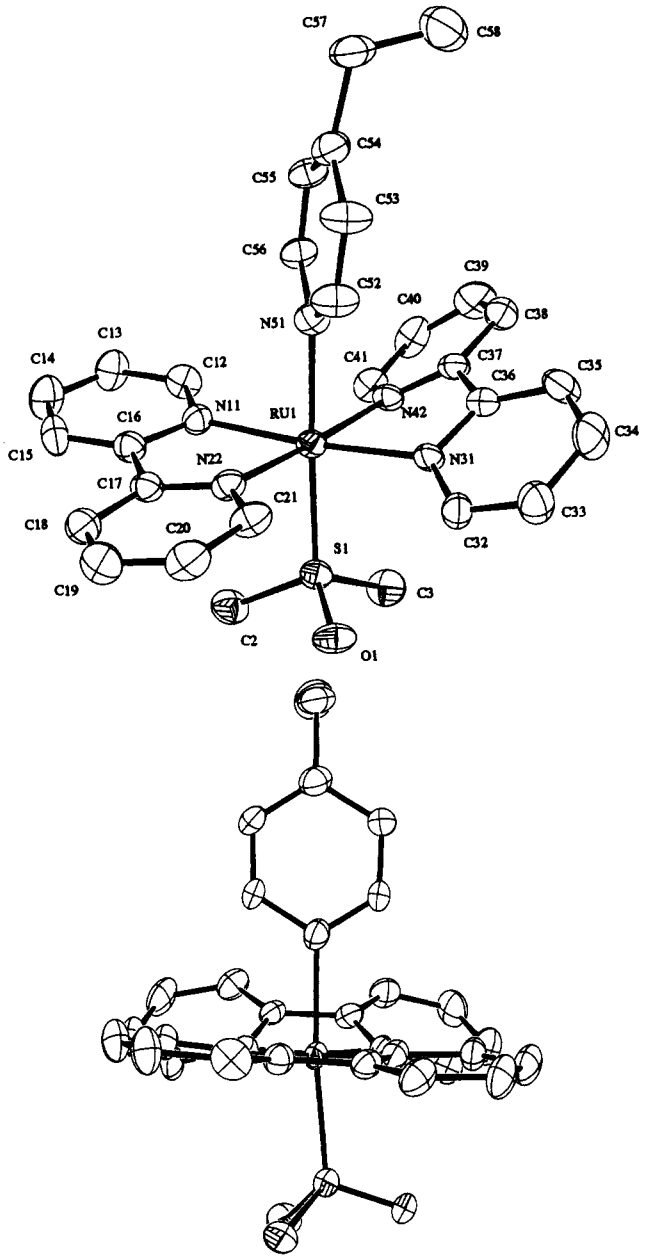

Figure 3. (a) Top: Structural representation of the cation of **2**, *trans*-$[Ru(bpy)_2(4\text{-Etpy})(DMSO)]^{2+}$, with hydrogen atoms omitted. The thermal ellipsoids correspond to 50% probability. (b) Bottom: Alternative view of the cation of **2**, *trans*-$[Ru(bpy)_2(4\text{-Etpy})(DMSO)]^{2+}$, perpendicular to the plane of the 4-Etpy ring.

SO)]$^{2+}$ which gives a clear picture of the coordination geometry. An alternative view perpendicular to the plane of the 4-ethylpyridine ring is shown in Figure 3b. The space group is the monoclinic $P2_1/c$ with four molecules in the unit cell. The trans stereochemistry of the bipyridine ligands can be clearly seen. To date, the authors are aware of a total of only five reported structures of salts of the type *trans*-$[Ru(bpy)_2(X)(Y)](Z)^n$. These are the Ru(III) salt *trans*-$[Ru(bpy)_2(OH_2)(OH)](ClO_4)_2$[14] and the Ru(II) salts *trans*-$[Ru(bpy)_2(PPh_3)_2](PF_6)_2$ (PPh_3 = triphenylphosphine),[28] *trans*-$[Ru(bpy)_2(PTZ)_2](PF_6)_2$ (PTZ = S-bound phenothiazine),[29] *trans*-$[Ru(bpy)_2(NO)Cl](PF_6)_2$,[30] and *trans*-$[Ru(bpy)_2(NO)OH](ClO_4)_2$.[31] Also published are the structures of the closely related bis(pyridine) salts *trans*-$[Ru(Me_2bpy)_2(py)_2](PF_6)_2$ (Me_2bpy = 4,4′-dimethyl-2,2′-bipyridine)[28] and *trans*-$[Ru(phen)_2(py)_2](PF_6)_2$ (phen = 1,10-phenanthroline).[32]

It is noteworthy that, of these structurally characterized Ru(II) salts, all but two are axially symmetrical derivatives of the form *trans*-$[Ru(L)_2(X)(Y)](PF_6)_2$ (L = bpy, Me_2bpy, phen; X = Y). This is in accord with the documented scarcity of such axially asymmetrical complexes owing to their generally problematic syntheses. Study of Figure 3a reveals a major difference between the orientation of the trans bpy ligands in the new complex **2** and in all of the structures previously reported. In complexes containing the *trans*-$[Ru(bpy)_2]^{n+}$ (n = 2, 3) moiety, varying degrees of twisted or bowed distortions are found which serve to reduce unfavorable interactions between the 6,6′-hydrogen atoms of the bpy ligands. However, in all cases these distortions are roughly symmetrical about the central Ru atom. Although ^1H NMR spectra show that in solution the two bpy ligands are equivalent, Figure 3a shows that in **2** these ligands undergo rather differing degrees of distortion. The dihedral angles are as follows: bpy^a–N_4 = 4.10°, bpy^b–N_4 = 27.50°, bpy^a–bpy^b = 24.59°.[33] Hence, bpy^b, which lies on the same side of the molecule as the methyl group of the 4-ethylpyridine ligand, is markedly bent toward the 4-Etpy ring and away from the DMSO ligand. The ligand bpy^a is bent toward the DMSO, but to a much lesser extent. Examination of crystal-packing diagrams does not serve to clarify why this should be the case, but it is likely to be due at least in part to the unusual asymmetrical coordination environment.

The other most interesting feature of the structure of **2** is the axial S-bound DMSO ligand. The Ru–S bond is of intermediate length at 2.257 Å, and the Ru atom is displaced by 0.089 Å out of the N_4 plane toward the DMSO. The shortest published value for a Ru(II)–S(O)Me_2 bond is 2.188 Å in $[Ru(NH_3)_5(DMSO)](PF_6)_2$,[15a] which represents a high degree of Ru–S π-back-donation resulting in a very strong interaction. This is possible because the five strongly basic ammine ligands cause a large build-up of available electron density at the Ru center. Much weaker Ru–S bonds are found in the complexes *trans*-$RuX_2(DMSO)_4$ of 2.360 Å for X = Br[15e] and 2.353 Å for X = Cl.[34] In both of these complexes, the bond in question is trans to another S-bound DMSO, which results in a competition for Ru π-electron density and hence gives considerably weaker bonds than those found in most other Ru(II)–DMSO complexes. In both of the complexes *cis*-$RuCl_2(DMSO)_4$[15c] and $[Ru(DMSO)_6](BF_4)_2$,[15d] Ru–S bond lengths of 2.252 Å have been reported for S-bound DMSO trans to O-bound DMSO. This is very similar to the value found in **2**, suggesting that the trans effect of 4-ethylpyridine is comparable to that of O-bound DMSO, which is considered a strong σ-donor ligand. However, this comparison is only partially valid since the nature of the equatorial ligands will also affect the electronic environment at Ru and hence the strength of the Ru–S interaction. The crystallographic observation of a relatively short Ru–S bond in **2** is in keeping with the empirical observation that the DMSO ligand is thermally difficult to displace (*vide supra*).

Also of interest in the structure of **2** is the S–O bond distance of 1.479 Å. Previous workers have established that the binding of DMSO to Ru(II) via the S atom causes an increase in the S–O bond order and hence a decrease in the bond distance compared to that found in free DMSO.[15a] Free DMSO has been found to have an S–O bond distance of 1.531 Å at 278 K,[35] but this is

(28) Cordes, A. W.; Durham, B.; Swepston, P. N.; Pennington, W. T.; Condren, S. M.; Jensen, R.; Walsh, J. L. *J. Coord. Chem.* **1982**, *11*, 251.
(29) Kroener, R.; Heeg, M. J.; Deutsch, E. *Inorg. Chem.* **1988**, *27*, 558.
(30) Nagao, H.; Nishimura, H.; Funato, H.; Ichikawa, Y.; Howell, F. S.; Mukaida, M.; Kakihana, H. *Inorg. Chem.* **1989**, *28*, 3955.
(31) Togano, T.; Kuroda, H.; Nagao, N.; Maekawa, Y.; Nishimura, H.; Howell, F. S.; Mukaida, M. *Inorg. Chim. Acta* **1992**, *196*, 57.
(32) Bonneson, P.; Walsh, J. L.; Pennington, W. T.; Cordes, A. W.; Durham, B. *Inorg. Chem.* **1983**, *22*, 1761.
(33) Definitions of planes: bpy^a = N(11),C(12),C(13),C(14),C(15),C(16),C(17),C(18),C(19),C(20),C(21),N(22); bpy^b = N(31),C(32),C(33),C(34),C(35),C(36),C(37),C(38),C(39),C(40),C(41),N(42); N_4 = N(11),N(22),N(31),N(42).
(34) Jaswal, J. S.; Rettig, S. J.; James, B. R. *Can. J. Chem.* **1990**, 1808.
(35) Reynolds, W. L. *Prog. Inorg. Chem.* **1970**, *12*, 1.

clearly of limited use for comparison with structures of complexes solved at 298 K. Nevertheless it has been established that, as the extent of Ru to S π-donation increases, the degree of shortening of the S–O bond is found to decrease. The reported range of S–O bond lengths for S-bound DMSO covers 1.527 Å in $[Ru(NH_3)_5(DMSO)](PF_6)_2$[15a] to 1.484 Å for *trans*-$RuBr_2(DMSO)_4$.[15e] A mean value of 1.482 Å is found in $[Ru(DMSO)_6](BF_4)_2$,[15d] and a mean value of 1.483 Å is found in *cis*-$RuCl_2(DMSO)_4$.[15c] That these values are very similar to that found in **2** is in accord with the similarities in Ru–S bond distances already noted. Figure 3b reveals that the DMSO is displaced slightly to one side in the direction of the O atom, giving a bond angle S–Ru–N(4-Etpy) of 174.79°. The DMSO molecule in **2** is approximately tetrahedral, as is usual for the S-bound mode.

The Ru–N bond distances found in **2** are typical of such compounds. The mean Ru–N(bpy) bond distance is 2.099 Å, and the Ru–N(4-Etpy) bond is slightly longer at 2.147 Å. The dihedral angle between the plane of the 4-Etpy ring[36] and the N_4 plane is 81.50°, as the 4-Etpy ligand is bent toward the more distorted bpy[b] ligand.

(36) Plane defined as N(51),C(52),C(53),C(54),C(55),C(56).

Conclusions

A novel strategy for the preparation of asymmetrically functionalized *trans*-$[Ru(bpy)_2]^{2+}$ complexes has been demonstrated in which simple pyridyl ligand bearing 4-substituents are introduced in a sequential fashion. This represents an approach which shows potential for extension to the introduction of more complex functionalized pyridyl ligands in order to create metallo–organic structures in which control of stereochemical properties is achieved. Current work is aimed at the utilization of this chemistry to synthesize stereochemically controlled chromophore-quencher and ligand-bridged complexes for study of photoinduced electron and energy transfer.

Acknowledgment. Support by the U.K. Science and Engineering Research Council under the NATO Postdoctoral Fellowship scheme and also the National Science Foundation (Grant CHE-9022493) is gratefully acknowledged. Also thanks are due to Dr. David W. Thompson for helpful suggestions.

Supplementary Material Available: Tables of hydrogen atomic parameters, bond distances and angles, and anisotropic thermal parameters (7 pages). Ordering information is given on any current masthead page.